



Improved corrosion protection for low carbon steel employed for oil tanks: Investigation of wear

Marwa Sulaiman*, Enas Muhi Hadi

Department of Applied Science, Material Science Division, University of Technology, Baghdad, Iraq

*) Email: marwa.s.jubair@uotechnology.edu.iq

Received 15/2/2025, Received in revised form 23/3/2025, Accepted 5/4/2025, Published 15/5/2025

In this research, by dipping technique, a new glass-ceramic coating on a substrate is applied and developed without prior surface chemical treatment as a single coat. For the low-carbon steel with 0.2% C, various glass frit mixture substrates have been selected at different dispersions and are utilized to acquire a glass-ceramics coating that contains the optimum coating features. The test results also indicated that the mechanical properties (hardness, wear rate) of the resultant coating have been greatly improved by both silicate dispersion supplements into the mixture frit for all cases. On this basis, it is found that the wear rate is less than 3.7134×10^{-7} g/cm that of the specimens coated with glass-ceramic coating (1.175×10^{-7} g/cm) and that of the base metal, and the hardness value of the glass-ceramic coating (560 HV) is enhanced greatly to reach (760 HV) at silicate dispersion in 700 °C for 120 min. The electrochemical corrosion test in 3.5% NaCl solution showed higher corrosion resistance for the specimen coated with a glass-ceramic (frit) mixture with zirconium 3.777×10^{-3} mm/y compared to the uncoated specimen 5.533×10^{-1} mm/y; the specimen coated with a glass-ceramic (frit) mixture with zirconia by dip coating is the best among all specimens.

Keywords: Carbon; Corrosion; wear.

1. INTRODUCTION

Ceramic nanomaterials are of great importance in the field of coatings due to their unique properties resulting from small particle size and increased surface area. They work to in several industrial applications, the higher surface hardness, low friction coefficient, and perfect wear resistance are the most common requirements of the machine components [1]. Due to its extensive fabrication features, low carbon steel is noted for its moderate strength and good machinability, making it a popular choice

in many manufacturing processes. However, to meet the demanding criteria of specific applications, it may require surface treatments or the addition of alloying elements to enhance its performance characteristics of ductility; it is employed for structural applications in ships, buildings, bridges, and automobiles [2]. In addition, its versatility allows for easy machining and welding, making it a preferred choice in various manufacturing processes. Furthermore, advancements in surface treatment technologies have enabled the enhancement of its properties, allowing low carbon steel to meet the demanding requirements of modern engineering applications', it is usual to enhance the properties of low carbon steel through various heat treatment processes, such as quenching and tempering. These processes can significantly improve its hardness and strength, making it suitable for more demanding applications while still maintaining a level of ductility that is essential for structural integrity. ly used for many manufacturing as well as industrial applications due to its low cost and their easy fabrication [3]. Because the material of oil tanks and pipes corrodes and wears, causing damage to the tanks and pipes and siting oil and raw materials, low carbon steel is used in oil tanks, crude oil, and oil pipelines. It also causes the transportation and export of crude oil and oil products to be stopped. It has a significant impact on the nation's economy. The major steel alloys problem utilized in various applications that include aggressive provision and towering temperature is the poor wear resistance, as in turbines, protecting oil pipelines and tanks, petroleum products, and power plant applications [3]. Nonetheless, there are a number of strategies to prevent corrosion, such as applying a protective coating, which is the suggested course of action for creating corrosion-resistant materials. It has an important role in creating a barrier between corrosive fluids and metal surfaces, as well as enhancing hardness and wear by altering the properties of the surface and creating a new transition area between the base metal and the deposited layer. By creating thin coatings on their surface that range in thickness from a few microns to several atomic layers, metals can be protected. Internal corrosion is a major issue in crude oil transmission pipelines [4]. Crude oil is not corrosive; nevertheless, it becomes corrosive when water and sediment are present. When water separates at the bottom and comes into touch with the pipe wall, the density of crude oil and water differs. The main elements influencing the flow velocity of internal corrosion While a low flow rate promotes water droplet separation and stagnation at the tube's bottom, which leads to pitting corrosion, a higher flow rate causes erosion corrosion by removing the tube's internal layers, particularly in the weld joint (due to excessive root pass penetration) and areas of impact or change in flow direction, like the valves [5-7]. Wear could be defined as destruction to a solid surface that results in the progressive loss of materials, either as a result of sliding with another contacting surface or as a result of chemical attack in corrosive/high temperature environments. Corrosion and wear in the oil industry and extending the life of oil preservation tanks and pipelines. Relying upon its quality, the wear could be one of the four kinds, viz., illustrated below:

- adhesive Wear,
- abrasive Wear,
- erosive Wear,
- corrosive Wear [8].

The exposure of surfaces to scratching as a result of the wear test leads to the material being exposed from the inside to cracks and scratches and thus reduces the hardness of the material, as hardness is an important property of the surfaces, and the surface's resistance to scratching means that it has high wear resistance, corrosion resistance, and high hardness. The term "hardness" refers to a material's resistance to abrasion, distortion, or indentation. The depth or materials mechanical properties is usually used to determine the hardness of a material [9]. The new technology used a variety of surface coating materials applied utilizing various deposit procedures, such as chemical vapor deposition, physical vapor deposition, and the dip-coating method, for various engineering and production applications [10]. The properties of glass-ceramic coating systems have seen remarkable improvements in recent years [11]. Glasses are made of amorphous or organized molecular components that lack structure. Glass-ceramic materials are crystalline solids made through carefully regulated glass diversification. The fundamental

advantage of glass ceramics is that they are as easy to make and shape as typical glass items while still possessing many of the ceramic’s desirable features (high level of strength, higher resistance to thermal shock, extra hardness, etc.). Thermal expansion is the other glass-ceramic quality that could be changed over a wide range (from negative value to positive value), which made them appropriate for a variety of applications, including veneers for the metal frame action of crowns, bridges, and inlays, as well as restorative dentistry [10]. At the end of the last century and the beginning of the new one, the concept of enhancing materials properties only at the surface, as an economic way of increasing quality, is leading to a large number of procedures for surface modifications, including all kinds of coatings at the micro- and nano-level [12]. In this research, a comprehensive study is presented on the corrosion of oil pipes and the possibility of protecting these pipes by coating them with a glass-ceramic material.

2. EXPERIMENTAL WORK

2.1 Material selection and specimen preparation

In this research, the material utilized is low carbon steel. This alloy’s chemical analysis is carried out by SPECTRO MAXX in State (the Iraqi Ministry of Industry and Minerals – State Company for Steel Industries). The elemental composition of the alloy employed in this study is tabulated in Table 1. The previous dipping process: specimens are cut off into suitable dimensions for each test and ground up to (60, 100, 120) grids of emery paper and then ished with ultrasonic in acetone for 30 min at 25°C.

Table 1 Chemical composition of metal substrates.

Element	C%	Si%	Mn%	P%	S%	Cr%	Mo%	Ni%	Al%	Cu%	Fe%
Sample	0.0438	<	0.280	0.0055	0.0224	0.0252	0.0037	0.0350	0.0124	0.0472	Bal.
Fe		0.0005									

2.2 Frit manufacturing

In this study, glass frit mixtures with six types of coating materials (A, B, C, D, E, and F) have been used. The six types of glass frit mixtures that are composed of reagent-grade chemicals are SiO₂, CaO, Al₂O₃, 2SiO₂, Na₂O, ZnO, MnO, PbO, and ZrO₂. Glass frit mixture powder is mixed in the same weight ratio using a magnetic stirrer for 2 hrs, then the slips are placed on the substrate and placed in the furnace at 700°C. Glass frit powders with chemical composition are tabulated in Table 2.

Table 2 Glass frit mixtures chemical composition.

Sample	Na ₂ O	Al ₂ O ₃	SiO ₂	K ₂ O	CaO	ZnO	PbO	ZrO ₂
A	4.54	7.32	50.32	4.40	6.90	5.44	7.33	0.31
B	5.48	9.12	52.92	4.07	4.49	0.16	1.17	0.13
C	7.13	9.81	58.20	8.41	6.42	2.11	2.16	0.26
D	7.26	10.77	62.55	7.33	6.14	2.12	2.30	0.31
E	6.16	6.82	51.54	0.21	0.37	0.17	34.01	0.09
F	6.17	7.76	46.44	1.45	4.25	2.43	28.85	0.0001

2.3 Preparation of enamel slip

The frit powder is then processed for application of the coating by combining it with specified grinder additives to generate a dense slurry termed "slip" that can be applied uniformly and thinly to clean metal objects using the dipping technique [9]. The rheological properties of the coating material slip are considered crucial for proper application of the coating on the substrate [4]. As indicated in figure (1), type of dispersants, three types of dispersants are utilized to make the suspension in this study, and the best among them is chosen to prepare the coating.

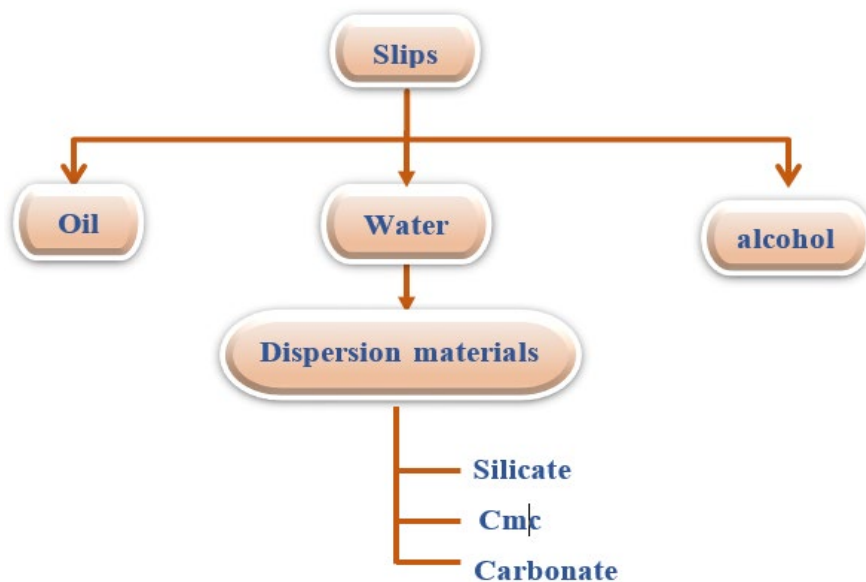


Figure 1 Types of dispersants.

2.4 Coating implementation

By dipping technique, the coating material has been applied on the metal substrate surface. This technique is considered very fast as well as not needing special plant. As illustrated in figure (2), the specimen has been dipped in solvent slip for 30 s, then withdrawn [13] and let to drain for 30 s (the specimen is held vertically and permitted for excessive slip to flow down). After the coating slip is applied on the surfaces of the specimen, in an oven the coated surfaces are dried for 15 min at 125°C to eliminate the specimen moisture. Then for 2 hours, it is fired at 700°C in an electrical furnace; also, the coating material reacts as well as fuses with the metal substrate surface to obtain a coating firmly adherent. Finally, to produce the glass-ceramic coating, it is left to cool slowly in the furnace [8]. Figure 2 shows the experimental procedure of the dipping method.

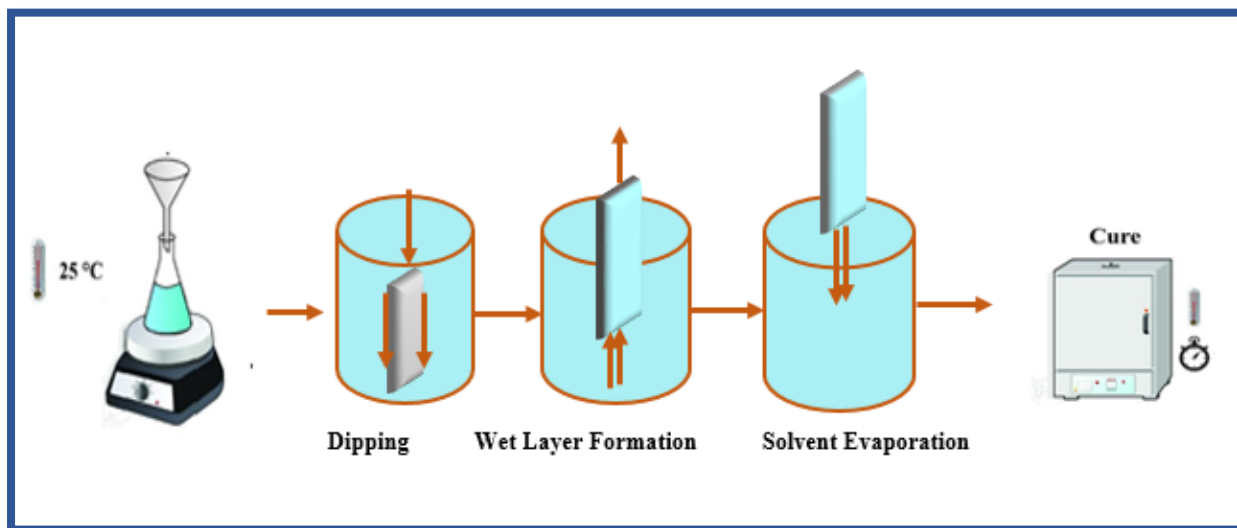


Figure 2 Dipping method.

2.5 Wear rate test

To calculate the specimens, wear rate, the weight method wear test is applied. Before and after the wear test, the specimens have been weighed by a sensitive balance type with four digits (max 250 g) within 0.0001 g accuracy. The loss of weight (ΔW^*) has been divided by the distance of sliding, and the wear rate is determined by the following equations [14, 15]:

$$\text{Wear rate} = \Delta W^*/Sd \quad \text{g/cm} \tag{1}$$

$$\Delta W^* = W1-W2 \tag{2}$$

W1, W2: specimen weight before and after the test (g).

$$Sd = 2\pi.r.n.t \tag{3}$$

Where Sd: represents the sliding distance (cm), r is radius from the specimen centre to the disc centre (cm).n is rotating disc number (r.p.m). t is sliding time (min).

To investigate the adhesive wear behaviour, a pin on disk machine that had been locally made and employed to prepare alloys after heat treatment is used under sliding dry conditions, then followed the ASTM G99-17 standard. Various loading and sliding speeds have been applied for 375 rpm and a sliding distance of 7 cm for various times; the rotating stainless-steel disk has been utilized. One of the important factors which play a significant role in wear rate is applied load. Severe wear appears at the high load levels and mild wear at the low load levels in wear tests under constant condition. Several experiments are carried out to observe the effect of normal load on wear rate, it is observed that wear rate increases with the increase of loads in most metal and alloys. With the increase in sliding speed, velocity and distance, the wear rate and cumulative wear loss increases for all the materials. The sliding speed influences the wear mechanism strongly and at low sliding speed, the wear rate of the composites is lower. This may happen because at high speed, the micro thermal softening of matrix material may take place, which further, lowers the bonding effect of the reinforced particles with that of matrix material.

The test is accomplished in the University of Technology/Department of Applied Science/Baghdad, Iraq. As illustrated in Figure 3.



Figure 3 Wear test device.

The wear test is carried out under dry sliding conditions with varying variables as follows:

- 1) Change the applied load for all specimens at constant sliding time and speed.
- 2) Change the sliding time for all specimens at a constant load and sliding speed.

Wear test variables as shown in Table 3.

Table 3 Primary Wear Test Variables

<i>Code</i>	<i>Sliding Speed (m/sec)</i>	<i>Time (min)</i>	<i>Load (N)</i>
Variable	Fixed	Fixed	Fixed
A, B, C, D, E, F	375	15	5

Table 4 Wear Test Variables.

Code	Sliding Speed (m/sec)	Time (min)	Load (N)
C	Fixed 375	Variable (5,10,15,20,30)	Fixed 5
		Fixed 15	Variable (5, 10,15)
D	Fixed 375	Variable (5,10,15,20,30)	Fixed 5
		Fixed 15	Variable (5,10, 15)

2.6 Micro - hardness test

Figure 4 shows the device that is used to measure all the specimen’s hardness: the microhardness Vickers tester. The loading time is about 15 sec, and the applied load is 1.96 N. Five indentations have been applied on each surface of the specimen, as well as the average readings have been taken to explore the Vickers hardness. The test has been carried out in the University of Technology/Department of Applied Science/Baghdad, Iraq. The base alloy macro-hardness is quantified by employing the Vickers hardness apparatus and computed by the formulas below [17,18].

$$HV = 1.8544 * P / dav^2 \tag{4}$$

Where: P is refers to the applied load (Kg) dav is The rhombus indentation average diameter in (mm) . HV is Vickers hardness (Kg / mm²). mm²).

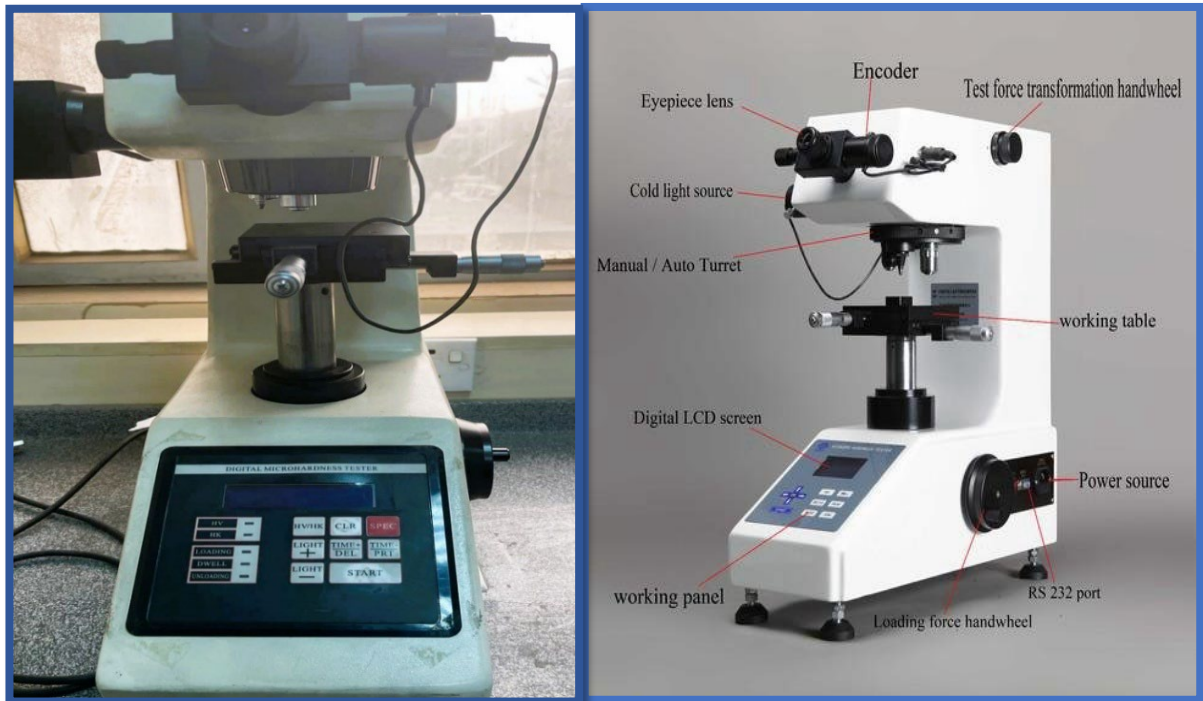


Figure 4 The device of Vickers micro hardness [19].

2.7 Corrosion tests

A test for corrosion is done on glass ceramics and bare surfaces coated spacemen in this work, including 3.5% NaCl (35 grams from NaCl in 1000 mL distilled water). the electrochemical cell consisting of three electrodes in a (1L) capacity: an electrode auxiliary, an electrode working, and a calomel electrode saturated.

2.7.1 Open circuit potential (OCP)

OCP measurements (also referred to as the equilibrium potential) are simply the potential difference between the working and reference electrode during immersion in the electrolyte at which there is no current applied.

2.7.2 Tafel polarization test

The linear Tafel sections of anodic and cathodic curves are extrapolated to corrosion potential to obtain the parameters of corrosion. Polarization is a mathematical technique used to estimate either the corrosion current (I_{corr}) or the corrosion potential (E_{corr}) in an electrochemical cell and to calculate the corrosion rate. The test is carried out at the Ministry of Science and Technology, Directorate of Materials Research. According to ASTM D6728, as shown in Figure 5, the corrosion test device is utilized.



Figure 5 Corrosion Test device.

3. RESULTS AND DISCUSSION

3.1 Wear rate measurement

Figure 6 illustrates the relationship between the rate of wear and the glass–ceramic coating used for coating the metal. The figure shows wear rate is conducted for all specimens (A, B, C, D, E, F) with the test conditions fixed as shows in the table (3) , where the results showed that C and D they are the best depending on the percentage of oxides that make up the glass frit mixtures as they contain the highest percentage of oxides of the elements (SiO_2 , Al_2O_3 , Na_2O , CaO , K_2O) that leads to reduce in the rate of wear for each (C,D) glass frit mixtures ,in addition, it is working to improve the properties of coating, As the glass-ceramic coating is generally resistant to chemical and mechanical properties and has high hardness, it gives surfaces the absence of cracks and pores. Since the hardness of the ceramic materials is higher than the hardness of the base metal, it resists wear instead of the material. The basis is that it is found that the wear rate is less than 3.7134×10^{-7} g/cm that of the specimens coated with glass-ceramic coating 1.175×10^{-7} g/cm and less than that of the base metal.

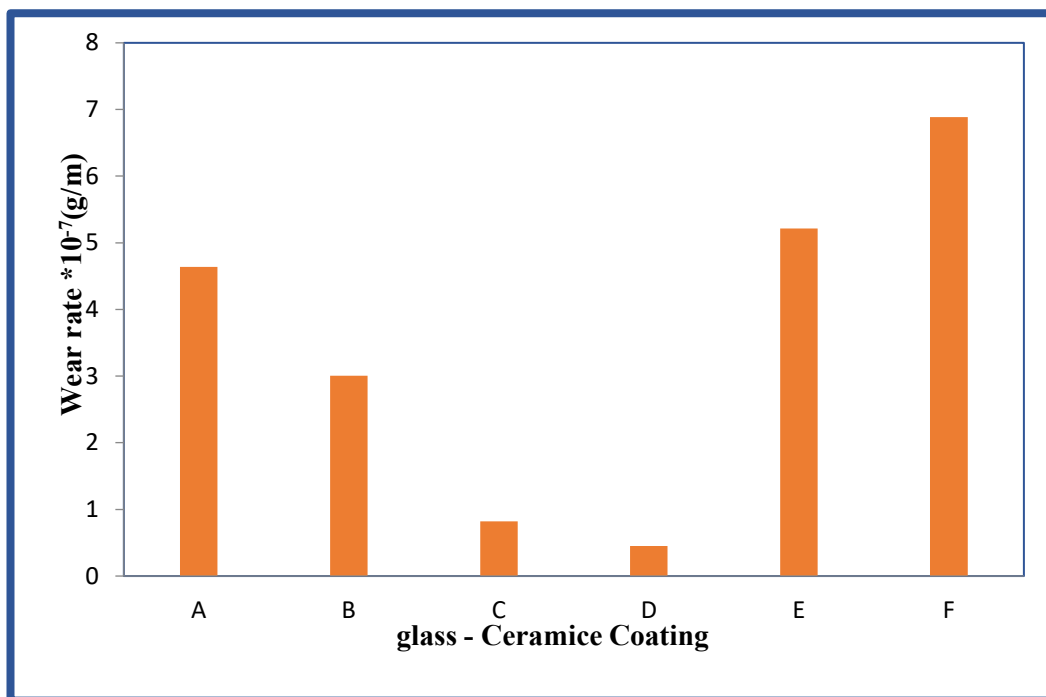


Figure 6 The wear rate vs glass - ceramics coating relationship.

Figure 7 (a, b, c, and d) depicts the wear rate and the glass-ceramics coating relationship that is used in metal coating for (C and D) specimens with changing test conditions as shown in Table 4. Figure 6 (a & b) showed the results of wear rate with the glass-ceramics coating at different loads (5, 10, 15) N and time at (15) min., and Figure 6. (c & d) showed the results of wear rate with the glass-ceramics coating at a different time (5, 10, 15, 220, 30) min and load at (5) N. The results showed a decrease in the wear rate at the glass-ceramics coating for the specimen (d) than (c) with the dispersion silicate sodium because silicate is very suitable as a dispersant for ceramic materials, and it is a ceramic material that accepts and interferes with glass-ceramics coating, then the carbonates sodium and CMC dispersant.

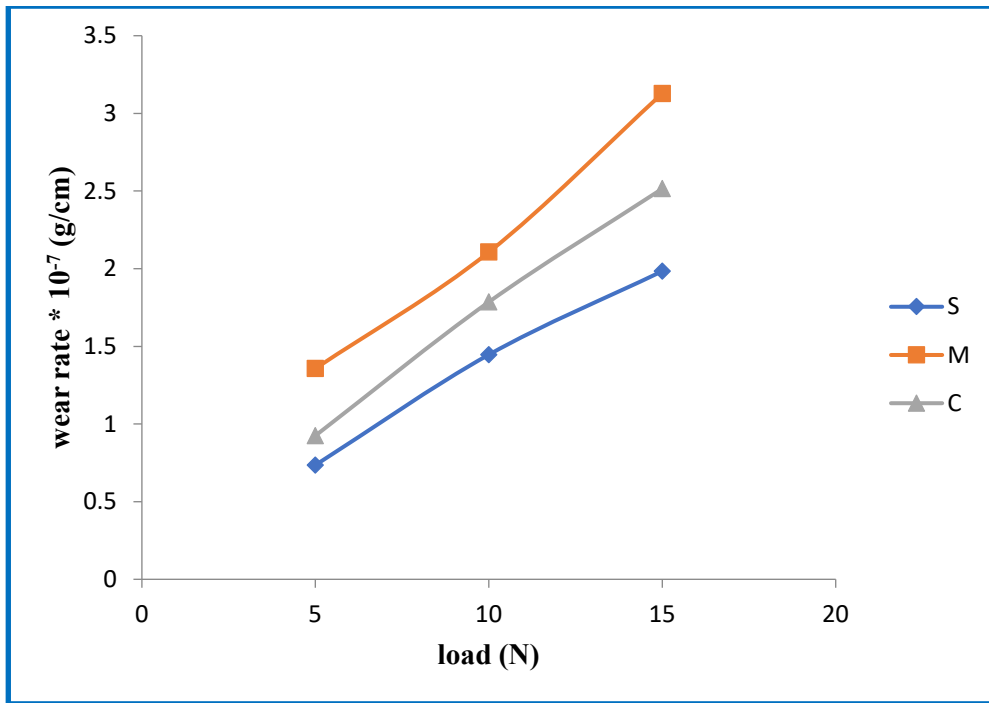


Figure 7 (a) The wear rate with the different load at specimen C at time 15 min.

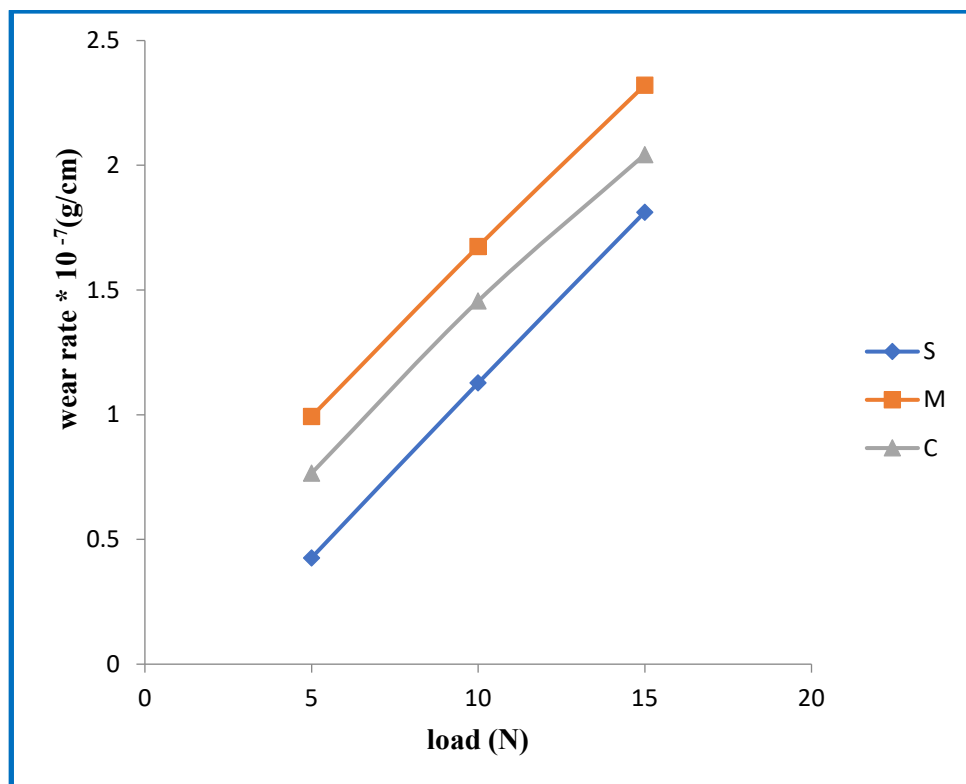


Figure 7 (b) The wear rate with the different load at specimen D at time 15 min.

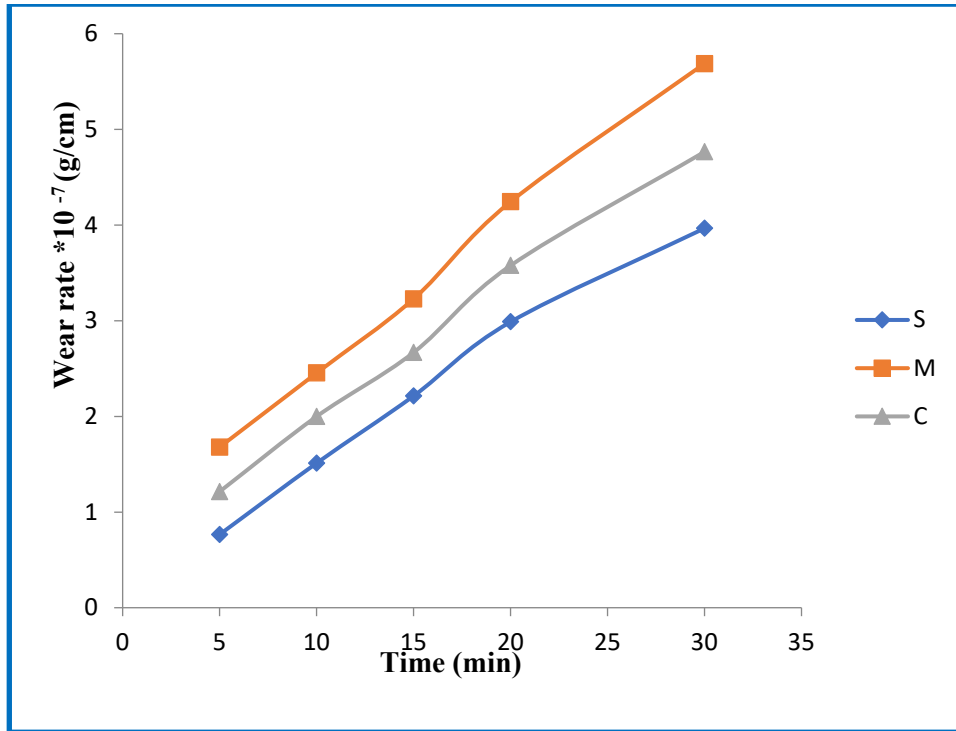


Figure 7 (c) The wear rate with the different time at specimen C at load 10 N .

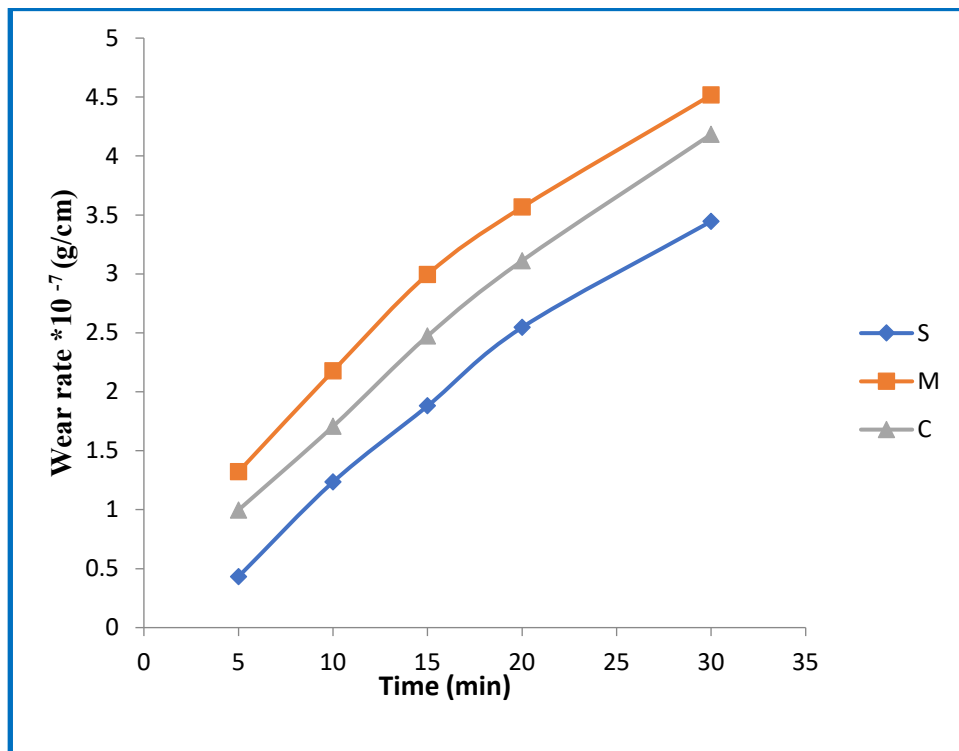


Figure 7 (d) The wear rate with the different time at specimen D at load 10 N.

3.2 Micro-hardness measurement

Figure 8 illustrates the micro-hardness and glass-ceramic coating relationship used for coating the metal. The figure shows Micro – Hardness is conducted for all specimens (A-F) with the test conditions where the results showed that C and D they are the best depending on the percentage of oxides that make up the glass frit mixtures as they contain the highest percentage of oxides of the elements (SiO_2 , Al_2O_3 , Na_2O , CaO , K_2O) which leads to increase in the Micro - Hardness of each (C,D) glass frit mixtures ,in addition, it is working to improve the properties of coating, As the glass-ceramic coating is generally resistant to chemical and mechanical properties and has high hardness, it gives surfaces the absence of cracks and pores. Since the hardness of the ceramic materials is higher than the hardness of the base metal.

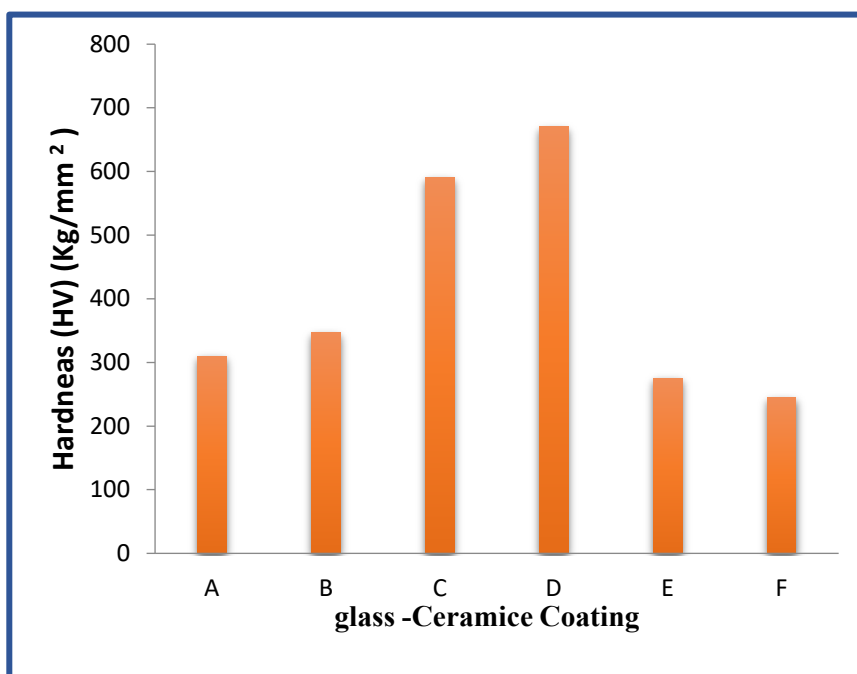


Figure 8 The relationship between hardness (HV) with glass - ceramics coating.

Figure 9 shows the effects of glass-ceramics coating on the micro-hardness values with different dispersants. It is clear from the figures that this increases the hardness value in the specimen (D) more than (C) at silicate sodium dispersant. This enhancement in the coating hardness is incorporating a greater percentage of a hard component (Na_2O , CaO , and K_2O) into the enamel. In addition, the silicate sodium dispersion is the best among the dispersants because it is compatible with the composition of glass, as it perfectly overlaps with glass mixtures and gives ideal properties for a smooth surface devoid of cracks and pores compared to the rest of the other dispersants used. It is also obvious from the figures that the hardness value of the glass-ceramics coating (560HV) is enhanced greatly to reach (760HV) at silicate dispersion in 700°C for 120 min.

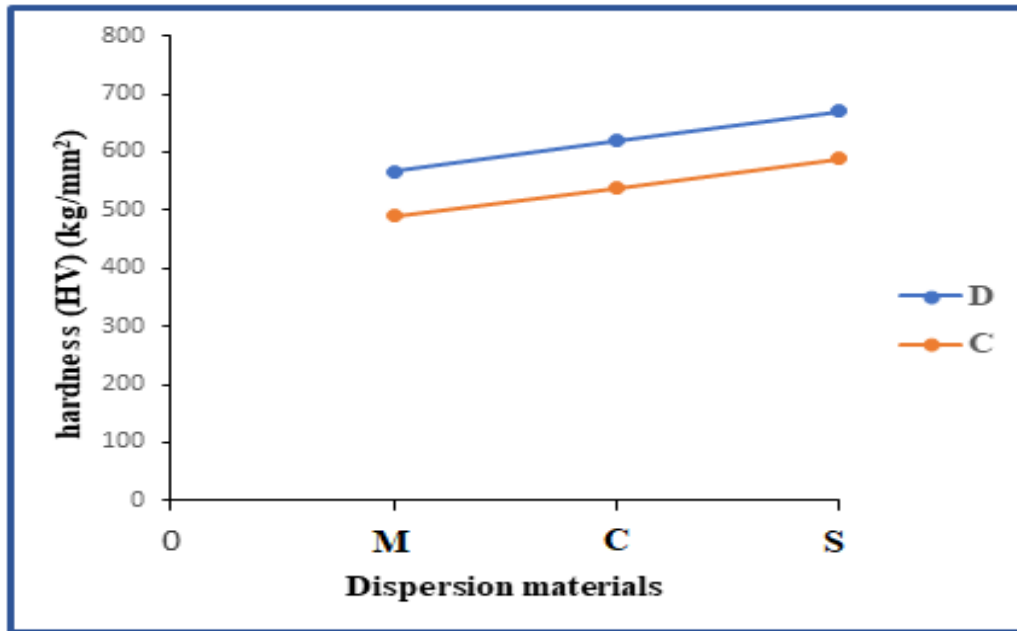


Figure 9 The relationship between hardness (HV) with the different dispersants at specimens (C & D).

3.3 Corrosion measurements

3.3.1 Open circuit potential (OCP) test

OCP test of low carbon steel substrate specimens in 3.5% NaCl solution shows an increase in passivation behavior with adding zirconia to the glass powder mixture, as shown in figures 10, where the OCP is -0.765 volts for the specimen (C with zirconia). Glass-ceramic (frit) mixture and -0.624 volts for specimen-coated (D with zirconia) glass-ceramic mixture, compared with -0.978 volts for uncoated specimens. Zirconia fills the pores in the coating layer, making it more retarding for corrosive ions to reach the specimen surface, which means the corrosive ions need more energy (potential) to reach the specimen surface.

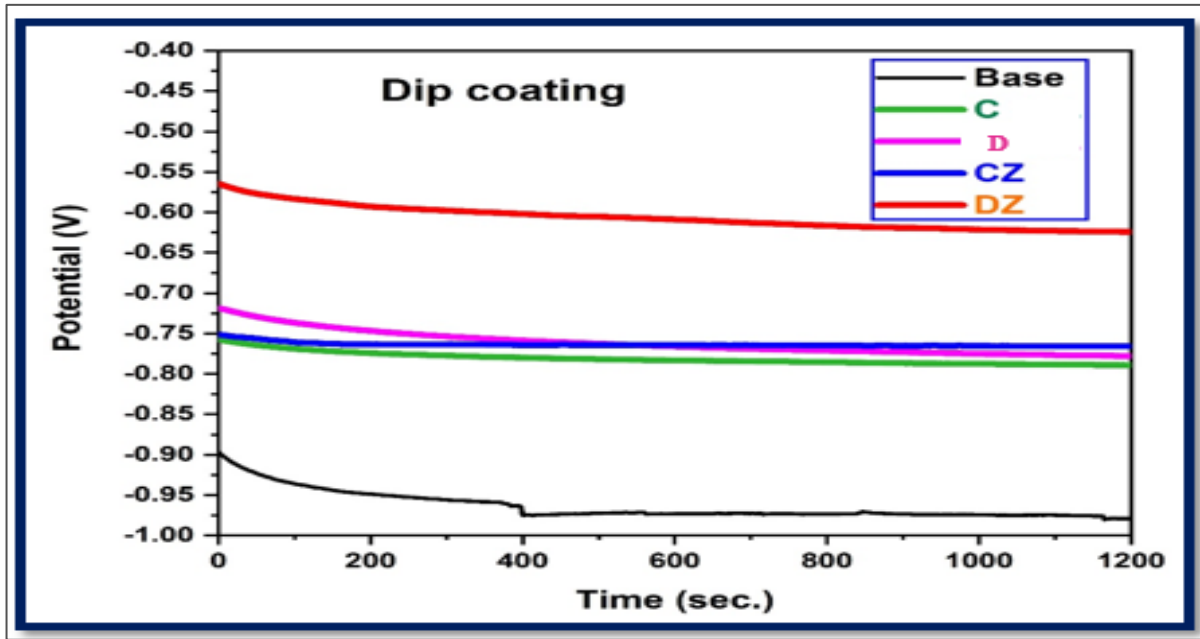


Figure 10 Open circuit potential results of low carbon steel specimens coated with different glass ceramic mixtures by a dip coating method.

3.3.2 Polarization curve (Tafel)

The polarization curve (Tafel) test shows a decrease in corrosion current and accordingly a decrease in corrosion rate for specimens coated with different glass ceramic mixtures by two methods: dip coating and flame thermal spray coating. Specimens coated with the dip coating method obviously show a high decrease in corrosion rate, especially for specimens coated with glass ceramic and zirconia, as shown in Figure 11 and Table 5. Where the corrosion rate for specimen coated (C with zirconia) glass-ceramic (frit) mixture is $5.258 \times 5.258 \times 10^{-3}$ mm/y and the corrosion rate for specimen coated (D with zirconia) glass-ceramic (frit) mixture is 3.777×10^{-3} mm/y, compared with 5.533×10^{-1} mm/y for uncoated specimen, that means we achieved a 105% reduction in corrosion rate for specimen coated (C with zirconia) glass-ceramic (frit) mixture and a 146% reduction in corrosion rate for specimen coated (D with zirconia) glass-ceramic (frit) mixture. All specimens coated by the dip coating method achieved a good reduction in corrosion rate compared with uncoated specimens.

Table 5 Corrosion characteristics extract from polarization curve (Tafel) for low carbon steel specimens coated with different glass ceramic mixtures by a dip coating method.

Glass – frit mixture coated layer	E corr. (volt)	I corr. (Amp/cm ²)	Measured area (cm ²)	Corr. Rate mm/y	βc V/dec	βa V\dc
uncoated	-0.891	5.437 × 10 ⁻⁵	1.125	5.533 × 10 ⁻¹	0.233	0.181
C	-0.770	4.845 × 10 ⁻⁶	1.125	4.841 × 10 ⁻²	0.205	0.362
D	-0.934	2.381 × 10 ⁻⁶	1.125	2.379 × 10 ⁻²	0.184	0.219
CZ	-0.916	5.262 × 10 ⁻⁷	1.125	5.258 × 10 ⁻³	0.171	0.266
DZ	-0.903	3.780 × 10 ⁻⁷	1.125	3.777 × 10 ⁻³	0.190	0.226

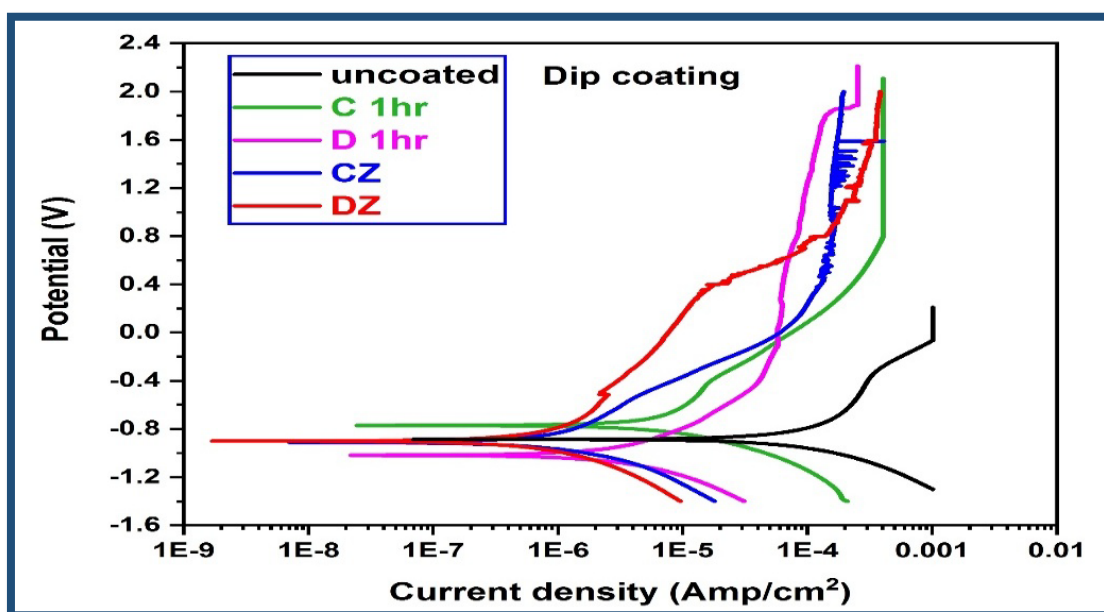


Figure 11 Polarization curve (Tafel) results of low carbon steel specimens coated with different glass ceramic mixtures by a dip coating method.

4. CONCLUSIONS

From the results obtained within this study, we could conclude that the specimen is C and/or D. In general, glass has good resistance to chemical and mechanical properties because the percentage of oxides (SiO₂, Al₂O₃, Na₂O, CaO, and K₂O) that are included in the composition gives surfaces the absence of cracks and pores and thus provides a glass–ceramic coating with high resistance because the presence of pores and cracks weakens the coating layer. Sodium silicate dispersion showed the same composition as glass and gives homogeneity and consistency to the coating and adhesion with the metal surface; other types of dispersants are less compatible with glass due to a difference in chemical composition. Specimen preparation conditions during firing in the presence of argon gas, which prevents oxidation and helps to obtain high cohesion between coating and metal. Corrosion tests prove that the specimens coated by the dip coating method have a higher OCP potential and lower corrosion rate for specimens coated (D) with zirconia glass-ceramic (frit) mixture.

Acknowledgments

The authors gratefully acknowledge the financial and technical support provided by the Applied Sciences Department, University of Technology, Baghdad-Iraq.

Funding

The authors declare that no funds, grants, or other support were received during the preparation of this manuscript.

Author contributions

All authors contributed to the study's conception and design. Marwa Sulaiman, and Enas M. Hadi performed material preparation, data collection, and analysis. Marwa Sulaiman wrote the first draft of the manuscript, and the author commented on previous versions of the manuscript. All authors read and approved the final manuscript.

Conflict of interest

The authors declare no competing interests.

Consent for publication

All the authors have been personally and actively involved in substantial work leading to the paper and consent to publish of the submitted paper.

Ethics approval

The paper reflects the authors' own research and analysis in a truthful and complete manner. The paper properly credits the meaningful contributions of co-authors and co-researchers. The results are appropriately placed in the context of prior and existing research. All the authors have been personally and actively involved in substantial work leading to the paper, and will take public responsibility for its content. This research doesn't involve human participants or animal.

Data availability

The datasets generated during and/or analyzed during the current study are available from the corresponding author upon reasonable request.

References

- [1] L. Umashanker, T.P. Bharathesh, R. Saravanan, *IJESC* 10 (2020) 26080
- [2] M. Sadeldine, *Exp. Theo. NANOTECHNOLOGY* 9 (2025) 1
- [3] S. Esmaeil, M. Nicolaie, J. Shrikant, *J. Therm. Spray Tech.* 28 (2019) 1749
- [4] S. Fayyadh, F. Mohammed, *J. Mech. Eng.* 20 (2023) 139
- [5] J. Esmaeil, *Russ. J. Electrochem.* 57 (2021) 663
- [6] J.T. Stephen, A. Adebayo, B.S. Oluwadare, *IJSTRE* 14 (2019) 1
- [7] A.H. Kadhum, M. Ahmed, *Int. J. Corros. Scale Inhib.* 10 (2021) 1812
- [8] H.A. Ali, A.M. Btihal, H.M. Jabbar, *Eng. Tech. J.* 32 (2014) 1472
- [9] M.S. Jassim, E.M. Hadi, *Int. J. Nanoelectron. Mater.* 15 (2022) 27
- [10] W. Hang, Z. Chuan, J. Chengyang, Z. Lijuan, C. Jiakai, H. Lihong, et al., *Crystals* 11 (2021) 346.

- [11] S. Pakhomova, Surface modification of low carbon steel to improve corrosion resistance, *MPMB* 963 (2020) 1
- [12] R. Nartita, I. Daniela, D. Ioana, *Sustainability* 13 (2021) 1
- [13] H.A. Ali, A.M. Ibtihal, H.M. Jabbar, *Eng. Tech. J.* 32 (2014) 1811
- [14] J.M. David, J. Juejun, C. Laurent, *Handbook of Glass*, Springer Nature Switzerland AG, 2019
- [15] S.M. Jiaad, S. Khansaa, A.H. Ahmed, *Eng. Tech. J.* (2021) 1632
- [16] M. Mohammed, *Kufa J. Eng.* 9 (2018) 131
- [17] M. Monika, Ł. Leszek, S. Paweł, T. Rolando, J. Candidato, A. Andrzej, *Mater. Sci. Nanotechnol.* 69 (2021) 1
- [18] D.S. Akeel, M. Adnan, Al-Khwarizmi *Eng. J.* 15 (2019) 63
- [19] N. M. Slaber, J. S. Kith, *Exp. Theo. NANOTECHNOLOGY* 9 (2025) 9